HOKKAIDO UNIVERSITY

Title	Hydrolysis-transglycosylation of sucrose and production of β-(2→1)-fructan by inulosucrase from Neobacillus drentensis 57N
Author(s)	Kido, Yusuke; Saburi, Wataru; Nagura, Taizo et al.
Citation	Bioscience biotechnology and biochemistry, 87(10), 1169-1182 https://doi.org/10.1093/bbb/zbad100
Issue Date	2023-07-25
Doc URL	https://hdl.handle.net/2115/92827
Rights	This is a pre-copyedited, author-produced version of an article accepted for publication in Bioscience biotechnology and biochemistry following peer review. The version of record Yusuke Kido, Wataru Saburi, Taizo Nagura, Haruhide Mori, Hydrolysis-transglycosylation of sucrose and production of β-(2→1)-fructan by inulosucrase from Neobacillus drentensis 57N, Bioscience, Biotechnology, and Biochemistry, Volume 87, Issue 10, October 2023, Pages 1169-1182, is available online at: https://doi.org/10.1093/bbb/zbad100.
Type	journal article
File Information	Kido2023BBB_NdIS.pdf

Hokkaido University Collection of Scholarly and Academic Papers : HUSCAP

Hydrolysis-transglycosylation of sucrose and production of β-(2→1)-fructan by inulosucrase from *Neobacillus drentensis* 57N

Yusuke Kido[1, 2], Wataru Saburi[2], Taizo Nagura[1], and Haruhide Mori[2]

[1]Research Center, Nippon Beet Sugar Mfg. Co., Ltd., Obihiro, Japan

[2]Research Faculty of Agriculture, Hokkaido University, Sapporo, Japan

Correspondence:

H. Mori, Research Faculty of Agriculture, Hokkaido University, Sapporo, Japan

E-mail: hmori@agr.hokudai.ac.jp

Running head

Characterization of *Neobacillus drentensis* 57N inulosucrase

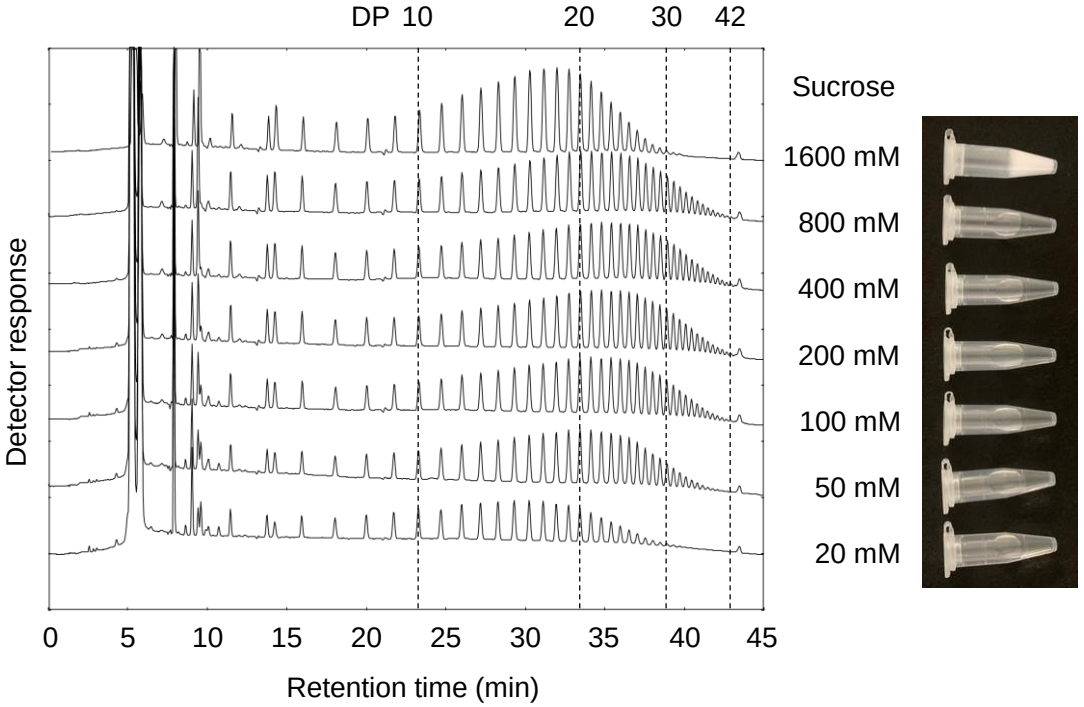
DP 10
20
30
42
Sucrose
1600 mM
800 mM
400 mM
200 mM
100 mM
50 mM
20 mM
Detector response
0
5
10
15
20
25
30
35
40
45
Retention time (min)

GA

ABSTRACT

Inulin, β-(2→1)-fructan, is a beneficial polysaccharide used as a functional food ingredient. Microbial inulosucrases (ISs), catalyzing β-(2→1)-transfructosylation, produce β-(2→1)-fructan from sucrose. In this study, we identified a new IS (NdIS) from the soil isolate, *Neobacillus drentensis* 57N. Sequence analysis revealed that, like other *Bacillaceae* ISs, NdIS consists of a glycoside hydrolase family 68 domain and shares most of the 1-kestose-binding residues of the archaeal IS, InuHj. Native and recombinant NdIS were characterized. NdIS is a homotetramer. It does not require calcium for activity. HPLC and ^{13}C-NMR indicated that NdIS catalyzed the hydrolysis and β-(2→1)-transfructosylation of sucrose to synthesize β-(2→1)-fructan with chain lengths of 42 or more residues. The rate dependence on sucrose concentration followed hydrolysis–transglycosylation kinetics, and a 50% transglycosylation ratio was obtained at 344 mM sucrose. These results suggest that transfructosylation from sucrose to β-(2→1)-fructan occurs predominantly to elongate the fructan chain because sucrose is an unfavorable acceptor.

Abbreviations

1-FFT, 2,1-fructan:2,1-fructan 1-fructosyltransferase; 1-SST, sucrose:sucrose 1-fructosyltransferase; ABC, ATP-binding cassette; BLAST, basic local alignment search tool; CFT, cycloinulooligosaccharide fructanotransferase; DDBJ, DNA Data Bank of Japan; DFA III, difructose anhydride III; DP, degree of polymerization; GH, glycoside hydrolase family; HPAEC-PAD, high-performance anion exchange chromatography-pulsed amperometric detection; HPLC, high performance liquid chromatography; IS, inulosucrase; NdIS, *Neobacillus drentensis* 57N IS; NMR, nuclear magnetic resonance; PAGE, polyacrylamide gel electrophoresis; PCR, polymerase chain reaction; SDS, sodium dodecyl sulfate; TLC, thin-layer chromatography

Graphical abstract

Chain length distribution of β-(2→1)-fructan synthesized at various sucrose concentrations by NdIS. Water-insoluble fructan was generated at 1,600 mM sucrose.

Keywords: inulosucrase; inulin; sucrose; *Neobacillus drentensis* 57N; glycoside hydrolase family 68

Introduction

Inulin is a polysaccharide, consisting of an average of 14–105 β-(2→1)-D-fructosyl residues (Pranznik and Beck 1985; Roberfroid 2005). It abundantly accumulates in plants, such as onion and *Asteraceae* plants, chicory and burdock (Niness 1999). It is resistant to human digestive enzymes, but is assimilated by beneficial intestinal bacteria; thus, it serves as a dietary fiber and prebiotic (Roberfroid and Slavin 2000). In addition, inulin functions as a gelation- and texture-adjusting agent. Thus, the use of inulin as a functional food ingredient has increased in recent years (Morris and Morris 2012; Shoaib *et al*. 2016). This polysaccharide is also a superior starting material for the production of fructooligosaccharides (Singh and Singh 2010), including difructose anhydride III (DFA III; Yokota *et al.* 1991).

In plants, inulin is synthesized by the action of two enzymes (Livingston *et al*. 2009). Sucrose:sucrose 1-fructosyltransferase (1-SST; EC 2.4.1.99) transfers the D-fructosyl moieties of sucrose to other sucrose molecules to produce 1-kestose (Fruβ2-1Fruβ2-1αGlc) (Edelman and Jefford 1968), and 2,1-fructan:2,1-fructan 1-fructosyltransferase (1-FFT; EC 2.4.1.100) catalyzes the D-fructosyl transfer reaction between β-(2→1)-fructan molecules to elongate some chains (Edelman and Jefford 1968; Vergauwen *et al.* 2003). Inulin-type β-(2→1)-fructans are produced by several

microorganisms (Olivares-Illana *et al*. 2002; Wada *et al*. 2003). In contrast to plant inulin biosynthesis, microbial β-(2→1)-fructan is synthesized by a single enzyme, inulosucrase (IS; EC 2.4.1.9), due to its transfructosylation from sucrose to both sucrose and β-(2→1)-fructan (Ponstein and van Leeuwen 1993). The structure of microbial β-(2→1)-fructans is diverse. For example, *Bacillaceae* fructans are linear, with a degree of polymerization (DP) in the range of 3–27 (Wada *et al.* 2003; Kralj *et al*. 2018; Yokoi *et al.* 2021), whereas lactic acid bacterial fructans are highly β-(2→6)-branched, with much higher DPs ($1 \times 10^4 – 4 \times 10^5$) (Rosell and Birkhed 1974; van Hijum *et al.* 2002; Anwar *et al*. 2008). Fructan synthesis by IS enzymes has also been reported in archaea (Kirtel *et al.* 2019). The archaeal enzyme InuHj from *Halalkalicoccus jeotgali* B3T catalyzes the production of water-insoluble inulin-type fructans from sucrose (Ghauri *et al.* 2021a).

In the sequence-based classification of carbohydrate-active enzymes (Drula *et al.* 2022), IS belongs to glycoside hydrolase family 68 (GH68). GH68 is composed of sucrose-specific D-fructofuraoside-acting enzymes, namely IS, levansucrase (EC 2.4.1.10), and β-fructofuranosidase (EC 3.2.1.26). GH68 enzymes catalyze the hydrolysis and transglycosylation of sucrose, with net retention of the anomeric configuration of the substrate, through a double-displacement mechanism involving the formation of a covalent bond intermediate (Chambert *et al*. 1974; Chambert and Gonzy-Treboul 1976; Hernandez *et al.* 1995; Song and Jacques 1999). The three-dimensional structure of the IS has been determined in the truncated active InuJ of the lactic acid bacterium *Lactobacillus johnsonii* (Pijning *et al*. 2011) and the archaeal InuHj (Ghauri *et al*. 2021b). The five-bladed β-propeller fold in the catalytic domain is common among GH68 enzymes. The residues involved in active site formation, including the three acidic catalytic residues that function as nucleophile, general acid/base catalyst, and transition-state stabilizer, located on the first-strands of blades 1 (1A), 4 (4A), and 3 (3A), respectively (Meng and Fütterer 2003; Yanase *et al.* 2002; Song and Jacques 1999; Batista *et al*. 1999), are mostly conserved in

GH68. In addition to the catalytic domain, ISs from lactic acid bacteria have additional domains at N- and C-termini (van Hijum *et al*. 2002; Olivares-Illana *et al*. 2002; Anwar *et al*. 2008). The C-terminal domain is involved in anchoring the enzyme to the cell wall (Rathsam *et al.* 1993; van Hijum *et al.* 2002), whereas the function of the N-terminal domain is unknown (del Moral *et al.* 2008). Most other bacterial ISs possess only a catalytic domain, but some enzymes have a short N-terminal domain (Kralj *et al.* 2018; Frasch *et al*. 2017; Yokoi *et al.* 2021).

Inulin is not only a functional ingredient, but also a starting material for the production of functional oligosaccharides. Demand for ISs with various specificities for β-(2→1)-fructans is increasing to expand the variety of β-(2→1)-fructans. In this study, we found that the soil isolate *Neobacillus drentensis* 57N extracellularly produced GH68 IS (NdIS), and described the functions of NdIS and the production of inulin-type polysaccharides, investigated using native and recombinant enzymes.

Materials and methods

Isolation of IS-producing strain 57N

Strain 57N was isolated from soil of grassy place in Hokkaido, Japan, on culture medium plates containing 20 g/L sucrose (Fujifilm Wako Pure Chemical, Osaka, Japan), 5 g/L phytone peptone (Becton Dickinson, Franklin Lakes, NJ, USA), 10 g/L yeast extract (Nacalai Tesque, Kyoto, Japan), 5 g/L KH_2PO_4, and 15 g/L agar (Nacalai Tesque). The pH of the culture medium was adjusted with NaOH to pH 7.2. The plates were incubated at 35°C for 24 h. Single colonies were isolated and cultured in the same liquid medium without agar at 35°C with shaking for 48 h. Inulin-type-fructan-producing activity was evaluated as follows. The culture supernatant (20 μL) was mixed with 100 μL of 400 mM sucrose in 40 mM MES-NaOH buffer (pH 6.5), and incubated at 37°C for 20 h (sample 1). A portion (40 μL) of

sample 1 was mixed with 2 μL (0.4 U) of endo-inulinase from *Aspergillus niger* (Novozym 960; Novozymes, Bagsværd, Denmark) and incubated at 35°C for 24 h (sample 2). Here, 1 U of endo-inulinase was defined as the amount of enzyme that produced 1 μmol of reducing sugar from 4 g/L inulin at 37°C and pH 6.5 in 1 min. The saccharides in samples 1 and 2 were analyzed by thin-layer chromatography (TLC). Sample 1 (20 μL) was subjected to digestion with recombinant levanase from *Bacillus* sp. (United States Biological, Salem, MA, USA) and dextranase from *Penicillium* sp. (Sigma Aldrich, St. Louis, MO, USA) under the same conditions as with endo-inulinase, but, at 0.5 U/mL in the reaction mixture.

TLC analysis

Samples containing 8.6 μg of saccharides were spotted onto a silica gel 60 plate (Merck, Darmstadt, Germany) and developed with the solvent, 2-propanol/1-butanol/water (2/2/1, v/v/v). Sugar spots were detected by spraying a detection reagent (H_2O/methanol/sulfuric acid [9/9/2, v/v/v]) and heating the plate at 105°C.

Identification of the bacterial strain

Chromosomal DNA from strain 57N, extracted using achromopeptidase (Fujifilm Wako Pure Chemical), was used as the template for polymerase chain reaction (PCR) to amplify the *16S rRNA* gene. Tks Gflex DNA Polymerase (Takara Bio, Kusatsu, Japan) and a primer set of 9F (5′-GAGTTTGATCCTGGCTCAG-3′) and 1510R (5′-GGCTACCTTGTTACGA-3′) (Nakagawa and Kawasaki 2001) were used. A Bigdye Terminator v3.1 Cycle Sequencing Kit (Thermo Fisher Scientific, Waltham, MA, USA) and primers 9F, 515F (5′-GTGCCAGCAGCCGCGGT-3′), 1099F (5′-GCAACGAGCGCAACCC-3′), 536R (5′-GTATTACCGCGGCTGCTG-3′), 926R (5′-

CCGTCAATTCCTTTGAGTTT-3′), and 1510R (Nakagawa and Kawasaki 2001) were used in the sequencing analysis. Sequencing was performed using an ABI Prism 3130xl Genetic Analyzer System (Applied Biosystems, Foster City, CA, USA) and Chromaspro version 2.1 (Technelysium, Tewantin, Australia). Sequence similarity searches and phylogenetic classifications were performed using ENKI (Techno Suruga Laboratory, Shizuoka, Japan), DB-BA (version 15.0; Techno Suruga Laboratory), GenBank, the DNA Data Bank of Japan (DDBJ), and the EMBL Nucleotide Sequence Database. Cells grown on LB agar medium (Becton Dickinson) containing 20 g/L agar were used for subsequent tests. Morphological observations were performed using an optical microscope (BX50F4; Olympus, Tokyo, Japan). Cells were stained with Feyber G Nissui (Nissui Seiyaku, Tokyo, Japan) for Gram staining. Carbohydrate utilization and enzyme activities were analyzed according to previously described methods (Barrow and Feltham 1993) using the API 20NE kit (bioMérieux, Lyon, France).

Production of NdIS in media containing various carbon sources

The culture medium used to isolate strain 57N, containing 20 g/L sucrose, D-glucose, or D-fructose as the carbon source, was used. *N. drentensis* 57N was grown in 50 mL of the medium with shaking at 130 rpm at 30°C for 24 h. From 1 mL of the culture aliquot, the supernatant and bacterial cells were separated by centrifugation at 8,000 × *g*. Bacterial cells were suspended in 200 μL of 10 mM MES-NaOH buffer (pH 6.5). Enzyme activity was measured using the standard activity assay method described below.

Production and purification of IS from *N. drentensis* 57N

N. drentensis 57N was cultured in 400 mL of culture medium containing 20 g/L sucrose with shaking at 130 rpm at 30°C for 24 h. The supernatant was obtained by centrifugation at 12,000 × *g* at

4°C for 20 min. Ammonium sulfate was added to the supernatant up to 70% saturation, and the sample was kept at 4°C for 24 h with stirring. The precipitate was collected by centrifugation, dissolved in 50 mL of 10 mM sodium phosphate buffer (pH 7.0), and dialyzed against the same buffer. The samples were loaded onto a Toyopearl DEAE 650M column (2.5 cm i.d. × 20 cm; Tosoh, Tokyo, Japan) equilibrated with 10 mM sodium phosphate buffer (pH 7.0). Non-adsorbed protein fractions eluted with equilibration buffer were collected, and up to 80 mM ammonium sulfate was added. This sample was subjected to a Toyopearl Butyl 650M column (2.5 cm i.d. × 10 cm; Tosoh), equilibrated with 10 mM sodium phosphate buffer (pH 7.0) containing 80 mM ammonium sulfate. Two activity peaks were eluted with a linear gradient of 80–0 mM ammonium sulfate in the same buffer (total elution volume, 400 mL) and further passage of the same buffer without ammonium sulfate. Active fractions from the first major high-purity peak were collected. The purity of the fractions was determined using sodium dodecyl sulfate-polyacrylamide gel electrophoresis (SDS-PAGE; Laemmli 1970). The collected sample was dialyzed against 10 mM sodium phosphate buffer (pH 7.0), and stored at -80°C.

Sequence analysis of *NdIS* and neighboring genes

Purified NdIS was transferred onto a polyvinylidene difluoride membrane (Immobilon-PSQ; Merck Millipore, Burlington, MA, USA) using a semi-dry electroblotting apparatus (Bio-Rad, Hercules, CA, USA). The protein band on the membrane was detected using Coomassie Brilliant Blue R-250 (Fujifilm Wako Pure Chemical) and then cut off and subjected to N-terminal amino acid sequence analysis using Protein Sequencer Procise 492HT (Perkin Elmer; Waltham, MA, USA). To determine the internal amino acid sequences, NdIS digests were prepared using lysyl endopeptidases. NdIS (70 μg) was dried *in vacuo* and dissolved in 24 mg of urea and 75 μL of 0.25 M Tris-HCl buffer (pH 8.9) containing 10 mM EDTA. Then, 1 μL of 1.17 mg/mL lysyl endopeptidase (Fujifilm Wako Pure

Chemical) was added, and the sample was incubated at 37°C for 20 h. Peptides were separated from the digests by reverse-phase high-performance liquid chromatography (HPLC) under the following conditions: sample injection volume, 50 μL; column, Capcell Pak C18 UG120 (4.6 mm i.d. × 150 mm; Shiseido, Tokyo, Japan); column temperature, room temperature; elution, linear gradient of 0–80% acetonitrile in 0.1% trifluoroacetic acid in 100 min; flow rate, 1 mL/min; and detection, A_{280}. Each peak was isolated, dried *in vacuo* and dissolved in 50 μL of 80% acetonitrile containing 0.1% trifluoroacetic acid, and the amino acid sequence was analyzed using Procise 492HT.

PCR was performed using the following degenerate primers designed based on the sequences of peptides 1 and 2: sense primer, 5′-AAYTGGGAYAAYAAYGGNTGGGA-3′ (Y: T or C; N: A, T, C, or G); antisense primer, 5′-GTNGGNGCRAANGTNCCNCCRAA-3′ (R: A or G). KOD FX (Toyobo, Osaka, Japan) was used as the DNA polymerase, and the genomic DNA of *N. drentensis* 57N was used as a template. The amplified DNA fragment (737 bp) was cloned into pBluescript II SK (Stratagene, La Jolla, CA, USA) and sequenced using universal primers. The flanking DNA fragments were amplified by nested PCRs using an LA PCR *in vitro* Cloning Kit (Takara Bio) and *Pst*I or *Eco*RI digests of the genomic DNA with cassette DNA attachment (Takara Bio) as templates. The primers used were universal, containing the cassette DNA sequence and the following *NdIS*-gene-specific primers: antisense primers (5′-CAGATGAACCCCGTTTTTATCCG-3′ and 5′-CAAAGGTTGTTTTCGCAATCCGC-3′) for the upstream region and sense primers (5′-CTTCCAGACCAGCAGGTAATCAGC-3′ and 5′-AACGAGCCGAAAGATGAGAACG-3′) for the downstream region. The cloning of DNA fragments and nucleotide sequence analyses were performed as described above. The DNA sequence determined in this study was deposited to DDBJ with accession number LC767464.

Multiple sequence alignment

The deduced amino acid sequence of NdIS was aligned with characterized GH68 enzymes using ClustalW 2.1 (Thompson *et al.* 1994) and depicted with ESPript 3.0 (Robert and Gouet 2014). The ISs used and their GenBank accession numbers were as follows: *H. jeotgali* B3T IS (InuHj), ADJ14334.1; *Salipaludibacillus agaradhaerens* WDG185 IS (InuO), ATN45518.1; *Alkalihalobacillus krulwichiae* JCM11691 IS (InuBK), ARK30072.1; *Streptomyces viridochromogenes* DSM 40736 IS (HugO), EFL36273.1; *L. johnsonii* NCC533 IS (InuJ), AAS08734.1; *L. gasseri* DSM20604 IS, ACZ67286.1; *L. reuteri* 121 IS, OJI11288.1; *L. reuteri* TMW 1.106 IS, CAL25302.1; *L. jensenii* JV-V16 IS, EFH30007.1; *Streptococcus mutans* GS-5 IS, AAA88584.1; *Weissella confusa* MBFCNC-2 (1) IS, ADB27748.1; *Leuconostoc citreum* CW28 IS, AAO25086.1; *Zymomonas mobilis* ATCC29191 β-fructofuranosidase (FF*Zm*), AFN56767.1; and *Z. mobilis* ATCC29191 levansucrase (LS*Zm*), AFN56768.1. The crystal structure of InuHj (Protein Data Bank entry, 7BJ5) was used for the secondary structure representation.

Preparation of recombinant NdIS

The *NdIS* gene was amplified by PCR using PrimeStar Max DNA polymerase (Takara Bio) and the following primers: 5′-GGAGATATACATATGGCGGAAATCAGTTCAGAT-3′ (sense) and 5′-GTGGTGGTGGTGGTGGCGATTTGCCCCAAATGG-3′ (antisense). The plasmid was cloned into a pET-22b vector (Novagen, Darmstadt, Germany) and the DNA inserts and flanking regions were sequenced. The expression plasmid was used to produce recombinant NdIS with a His_6 tag at the C-terminus of the complete NdIS sequence. A transformant of *E. coli* BL21 (DE3) harboring the expression plasmid was cultured in 500 mL of LB medium containing 100 μg/mL ampicillin at 37°C until the A_{600} reached 0.5. Isopropyl β-D-1-thiogalactopyranoside (Fujifilm Wako Pure Chemical) was

added to a concentration of 0.1 mM, and the incubation was continued at 18°C for 18 h with vigorous shaking. The *E. coli* cells were harvested by centrifugation (5,000 × *g*, 4°C, 10 min), suspended in 10 mL of 10 mM sodium phosphate buffer (pH 7.5), and disrupted by sonication using a Sonifier 450 instrument (Branson; Danbury, CT, USA). The supernatant, obtained by centrifugation (12,000 × *g*, 4°C, 10 min), was loaded onto a Ni^{2+}-immobilized Chelating Sepharose Fast Flow column (2.5 cm i.d. × 6 cm; GE Healthcare, Uppsala, Sweden), which was pre-equilibrated with 10 mM sodium phosphate buffer (pH 7.5). After thoroughly washing the column with a buffer containing 50 mM imidazole, the adsorbed protein was eluted using a linear gradient of imidazole (50–300 mM, total elution volume, 400 mL). Fractions containing highly purified enzymes were collected and dialyzed against 10 mM sodium phosphate buffer (pH 7.0). The purified enzyme was stored at -80°C.

Protein assay

The protein concentrations of the purified samples were determined using the UV method (Mach *et al.* 1995). The concentration of purified enzyme was determined by amino acid analysis (Moore and Stein 1948). The molar concentration of the enzyme was calculated from the quantities of each amino acid after acid hydrolysis of the enzyme in 6 M HCl at 110°C for 24 h. Amino acid analysis was performed using a JLC-500/V amino acid analyzer (JEOL, Tokyo, Japan).

Blue native PAGE

The molecular mass of NdIS under non-denaturing conditions was determined by blue native PAGE (Schägger *et al.* 1994). Analytical samples were prepared using a Native PAGE Sample Prep Kit (Life Technologies, Carlsbad, CA, USA). Novex Native PAGE 4–16% Bis-Tris Gels (Life Technologies) were used, and electrophoresis was performed at a constant voltage of 150 V for 115 min

on ice. The Native Mark Unstained Standard (Life Technologies) was used as the molecular size standard.

Standard enzyme activity assay

The D-glucose-releasing activity toward sucrose was measured. A reaction mixture (100 μL), consisting of 80 mM sucrose, 40 mM MES-NaOH buffer (pH 6.5), 0.2 g/L bovine serum albumin (BSA; Fujifilm Wako Pure Chemical), and an appropriate concentration of enzyme, was incubated at 37°C for 10 min. The reaction was terminated by adding 20 μL of 0.5 M NaOH. Liberated D-glucose was measured using an F-kit, D-glucose/D-fructose (Roche Diagnostics, Basel, Switzerland). One unit of IS activity was defined as the amount of enzyme yielding a D-glucose- releasing rate of 1 μmol/min under these conditions.

Effects of pH, temperature, and metal ions on the activity and stability of NdIS

To determine the optimum pH and temperature, a standard activity assay was used, but 40 mM Britton-Robinson buffer (pH 3.0–12.0; a mixture of 40 mM acetic acid, 40 mM phosphoric acid, and 40 mM glycine, to which 200 mM NaOH was added to adjust the pH) was used for the reaction buffer, and various temperatures (30–65°C) were used. For pH stability measurements, 0.23 mg/mL of the enzyme was kept in 80 mM Britton-Robinson buffer (pH 4.1–11.0) at 4°C for 24 h, and residual activities were measured. To assess temperature stability, 4.7 μg/mL of the enzyme was kept in 10 mM MES-NaOH (pH 6.5) at 30–65°C for 15 min. The effects of metal ions were measured in the presence of 10 mM LiCl, NaCl, KCl, NH_4Cl, $MgCl_2$, $CaCl_2$, $CoCl_2$, and $NiCl_2$ under standard conditions. For recombinant NdIS, the optimal temperature, temperature stability in the presence of 10 mM $CaCl_2$, and enzyme activity in the presence of 10 mM EDTA were evaluated.

Kinetic parameters of the reaction with sucrose

The velocities of D-glucose and D-fructose release (aglycone release rates [v_{ag}] and hydrolysis rates [v_h], respectively) were measured under standard activity assay conditions, but with 1–800 mM sucrose. NdIS was 10.1 nM. Products were quantified using F-kit D-glucose/D-fructose. Transglycosylation rates (v_{tg}) were calculated by subtracting v_h from v_{ag}.

Data analysis was performed using nonlinear regression, based on the kinetic model shown in Fig. 1. The rate equations used were as follows (Bruker *et al.* 1999; Kawai *et al.* 2004; Kobayashi *et al.* 2011).

$v_{ag} = (k_{cat2}[S]^2 + k_{cat1}K_{m2}[S])/([S]^2 + K_{m2}[S] + K_{m1}K_{m2})$, (Eq. 1)

$v_h = k_{cat1}K_{m2}[S]/([S]^2 + K_{m2}[S] + K_{m1}K_{m2})$, (Eq. 2)

$v_{tg} = k_{cat2}[S]^2/([S]^2 + K_{m2}[S] + K_{m1}K_{m2})$, (Eq. 3)

The four kinetic parameters were expressed according to the rate constants shown in Fig. 1.

$K_{m1} = k_3(k_{-1} + k_2)(k_{-4} + k_5)/\{k_4k_5(k_{-1} + k_2) + k_1(k_{-4} + k_5)(k_2 + k_3)\}$

$K_{m2} = \{k_4k_5(k_{-1} + k_2) + k_1(k_{-4} + k_5)(k_2 + k_3)\}/k_1k_4(k_2 + k_5)$

$k_{cat1} = k_1k_2k_3(k_{-4} + k_5)/\{k_4k_5(k_{-1} + k_2) + k_1(k_{-4} + k_5)(k_2 + k_3)\}$

$k_{cat2} = k_2k_5/(k_2 + k_5)$

The transglycosylation ratio r_{tg} was defined as follows:

$r_{tg} = v_{tg}/v_{ag} \times 100 = [S]/(K_{TG} + [S])$, (Eq. 4),

where K_{TG} ($= k_{cat1}K_{m2}/k_{cat2}$) is the substrate concentration that provides a 50% transglycosylation ratio.

Analysis of transglycosylation in the initial reaction of NdIS

Reaction samples were prepared according to the standard activity assay using 800 mM sucrose

and 50.4 nM NdIS. Aliquots (100 μL each) were taken from the reaction mixture (1 mL), and the reaction was terminated at the indicated times. The samples were appropriately diluted with water and analyzed using high-performance anion exchange chromatography-pulsed amperometric detection (HPAEC-PAD), as described below.

Preparation of polysaccharides synthesized from sucrose by purified NdIS

A reaction mixture (10 mL) consisting of 400 mM sucrose, 40 mM MES-NaOH buffer (pH 6.5), and 504 nM NdIS was incubated at 37°C for 20 h. TLC analysis was performed as described above and HPAEC-PAD analysis was performed as described below. Two volumes of ethanol (-20°C) was added to the reaction mixture (10 mL) to precipitate the polysaccharide. After overnight incubation at 4°C, the precipitate was collected by centrifugation at 4°C at 12,000 × *g* for 5 min, washed thoroughly with 50% ethanol, and lyophilized.

To determine the effects of sucrose concentration on polysaccharide production, the reaction conditions were the same as above; however, 20–1,600 mM sucrose and recombinant NdIS (1.26 nM per 1 mM sucrose) were used. The samples were appropriately diluted with water and analyzed using HPAEC-PAD and HPLC, as described below.

^{13}C-nuclear magnetic resonance (NMR) analysis of the polysaccharide products of NdIS

The lyophilized polysaccharides produced by NdIS, inulin from chicory (Raftiline HP; Beneo-Orafti SA, Tienen, Belgium), and levan from *Z. mobilis* (Sigma Aldrich) were dissolved in 99.9% D_2O (Sigma Aldrich) at approximately 10 g/L. ^{13}C-NMR was performed at 27°C using a Bruker Advance Neo instrument (126 MHz; Bruker, Billerica, MA, USA).

Evaluation of the average DP of the polysaccharide products of NdIS

The concentrations of sucrose, D-glucose, and D-fructose in the reaction mixtures of recombinant NdIS and 20–1,600 mM sucrose were measured using HPLC. The HPLC conditions were as follows: Sugar KS-801 column (8.0 mm i.d. × 300 mm; Shodex, Tokyo, Japan) at 60°C and 50 μM NaOH as the eluent at a flow rate of 1.0 mL/min. The refractive index was monitored and 5 g/L sucrose, D-glucose, and D-fructose solutions were used as quantification standards. Because the average number of D-fructosyl residues transferred from sucrose was calculated from the ratio of the sucrose concentrations used as the donor and acceptor, the average DPs of the inulin-type polysaccharides was calculated using the following equation:

$$\text{Average DP} = 2 + ([\text{Glc}] - [\text{Fru}])/([\text{Suc}]_0 - [\text{Suc}] - [\text{Glc}]),$$

where [Suc], [Glc], and [Fru] are the molar concentrations of sucrose, D-glucose, and D-fructose, respectively, measured in the reaction mixtures and $[\text{Suc}]_0$ denotes the initial sucrose concentration.

HPAEC-PAD analysis

Transglycosylates produced in the early stage of the reaction were analyzed using a Dionex ICS-3000 equipped with CarboPac PA1 (4 mm i.d. × 250 mm; Thermo Fisher Scientific) under the following conditions: sample injection, 5 μL; column temperature, room temperature; flow rate, 1 mL/min; detection, pulsed amperometry; and mobile phase, 150 mM NaOH containing sodium acetate (25 mM, 0–1 min; 25–50 mM, 1–2 min; 50–200 mM, 2–20 min). D-glucose, D-fructose, sucrose, fructooligosaccharides (1-kestose, nystose, and fructosylnystose; Fujifilm Wako Pure Chemical), and inulin from chicory (Raftiline ST; Beneo-Orafti SA) (40–200 μM, 5 μL) were used as standards. For the analysis of polysaccharide DP, elution was performed using a linear gradient of 0–600 mM sodium acetate in 100 mM NaOH as the mobile phase for 60 min.

Results

Isolation of inulin-type polysaccharide synthesizing bacterium from soil

Strain 57N, isolated from soil, exhibited a cream-colored, round-shaped colony morphology on a sucrose-containing agar-based medium. In the liquid fermentation supernatant, activity producing an inulin-type polysaccharide from sucrose was observed (Fig. 2a). In addition to residual sucrose, polysaccharides that did not migrate from the origin of the TLC were detected in the TLC analysis of the reaction mixture. This polysaccharide was digested to D-fructose by an endo-inulinase similar to authentic inulin (Fig. 2a), but not by levanase and dextranase (data not shown).

The partial *16S rRNA* gene sequence of strain 57N was 99.6% identical to the *16S rRNA* gene sequence of *Neobacillus drentensis* LMG21831 (GenBank accession number, AJ542506.1). Physiological tests revealed that strain 57N is a non-motile Gram-positive rod (1.0–1.2 × 2.5–4.0 μm) that grows below 50°C under aerobic and anaerobic conditions. This strain was capable of spore formation. Carbohydrate utilization and enzymatic activity were almost consistent with those of *N. drentensis* LMG21831 (Heyrman *et al*. 2004). Therefore, strain 57N was identified as *N. drentensis* and named *N. drentensis* 57N.

Purification and basic properties of native NdIS

The growth of *N. drentensis* 57N and its enzyme production were tested in a shake flask culture with liquid media containing sucrose, D-glucose, and D-fructose as carbon sources. It grew well in all media, but NdIS activity (3.4 U/mL culture) resulting in the release of D-glucose from sucrose was only found in the supernatant of the culture using sucrose-containing medium. No detectable activity (< 0.076 U/mL culture) was observed in other supernatants or cell suspensions.

NdIS (7.2 mg) was purified to homogeneity from 400 mL of the culture supernatant of *N. drentensis* 57N by ammonium sulfate precipitation and two-column chromatography, with a 22% yield of activity. In hydrophobic column chromatography, two activity peaks were observed in the adsorbed fractions (Supplementary Fig. 1). NdIS was obtained from the first active peak. Preliminary analysis of the reaction products and protein sequences suggested that the second active peak contained another IS-like enzyme. This will be described elsewhere after complete purification. The specific activity of the purified NdIS enzyme in the presence of 80 mM sucrose at 37°C was 38.4 U/mg. Purified NdIS showed a single protein band of 44 kDa on SDS-PAGE and 174 kDa on blue native-PAGE (Fig. 3). This indicated that NdIS is a homotetrameric protein. NdIS exhibited the highest activity at pH 6.1 and 45°C. More than 90% of its original activity was retained after incubation in a pH range of 5.1–7.5 at 4°C for 24 h and at 45°C or lower temperature at pH 6.5 for 15 min. The NdIS activity decreased to 51% and 35% in the presence of 10 mM $CoCl_2$ and $NiCl_2$, respectively, and increased to 112% in the presence of 10 mM $CaCl_2$. The monovalent cations tested had no effect on NdIS activity (Table 1).

Polysaccharides were produced by incubation with 400 mM sucrose and purified NdIS. They were detected as a non-migrating spot on TLC and they were almost completely degraded by the endo-inulinase (Fig. 2a). In the HPAEC analysis of native NdIS reaction products, saccharides up to an approximate DP of 42 were detected at the same retention times as inulin (Fig. 2b). Polysaccharides were recovered from the reaction mixture via ethanol precipitation. The ^{13}C-NMR spectrum was in good agreement with that of authentic inulin, but not with that of levan (Fig. 2c). These results indicated that the NdIS product was an inulin-type β-(2→1)-fructan.

Sequence analysis of NdIS

Partial amino acid sequences of NdIS derived from its N-terminus and five peptides from lysyl-

endopeptidase digests were determined (Fig. 4a, underlined). Using PCR, a 4,206-bp-long DNA fragment, containing the 1,332-nt-long *NdIS* gene, was generated (Fig. 4b). The *NdIS* gene encoded a protein comprising 443 amino acids. It contained all of the determined partial amino acid sequences (Fig. 4a). The N-terminal sequence of purified NdIS was identical to that of Ala33–Trp43 in the deduced sequence. The SignalP-5.0 program (Armenteros *et al.* 2019) suggested that the N-terminal Met1–Ala32 is a signal peptide. Therefore, the 32-residue-long N-terminal region was regarded as the signal sequence used for secretion, and the mature NdIS was composed of 411 residues. The calculated molecular mass of the mature NdIS (45.9 kDa) matched well with the mass (44 kDa) measured by SDS-PAGE (Fig. 3). A sequence similarity search using the BLAST program (Altschul *et al.* 1990) indicated that NdIS was 99.8% identical to a putative GH68 fructosyltransferase from *Bacillus* sp. AFS031507 (NCBI, WP_098930566.1), encoded by a member of this gene cluster (Fig. 4c). NdIS also showed high sequence identity with the following characterized GH68 IS enzymes: 68% identity with *S. agaradhaerens* InuO, 66% with *A. krulwichiae* InuBK, and 37% with *S. viridochromogenes* HugO. It also showed sequence similarity to two IS enzymes with known ternary structures. The overall NdIS sequence showed 33% identity with InuHj from the archaeon *H. jeotgali* B3T and 14% identity with the catalytic domain of InuJ (Ala180–Gln707) from *L. johnsonii*. This similarity indicated that NdIS is a member of GH68 and is composed solely of a catalytic GH68 domain. No extra domains, such as the N-terminal variable domain or the C-terminal cell-wall-anchoring domain of ISs from *L. johnsonii* and other lactic acid bacteria were found in the NdIS sequence. Partial amino acid sequence alignments of the GH68 enzymes, NdIS, characterized ISs, and two non-IS enzymes (β-fructofuranosidase and levansucrase from *Z. mobilis* ATCC29191, FF*Zm* and LS*Zm*, respectively) are shown in Fig. 5. This alignment suggests that the three possible catalytic residues acting as nucleophile, general acid/base, and transition-state stabilizer of NdIS are Asp77, Glu317, and Asp233, respectively. In addition, most of

the other residues involved in the formation of subsites −1 to +2 of the archaeal IS InuHj are conserved in NdIS (His112, Ala148, Arg232, His335, and Asn398). Glu266 of InuHj, hydrogen-bonded to the D-glucosyl and D-fructofuranosyl moieties in subsite +1, was not conserved, but corresponded to Gln315 in NdIS. His112 of NdIS is equivalent to and corresponds to His79 of FF*Zm* and Asn84 of LS*Zm*. A mutagenesis experiment suggested that the His residue in this position is crucial for the β-(2→1)-linked substrate preference (Okuyama *et al.* 2021). These residues comprising subsites −1 to +2 in NdIS were more similar to ISs from non-lactic acid bacteria, and even to FF*Zm* and LS*Zm*, than to ISs from lactic acid bacteria. The residues constituting the Ca^{2+}-binding site 1 of *L. johnsonii* InuJ, Asp419, Gln450, Trp487, Asn489, and Asp521, were not conserved in the NdIS sequence, except for the Asn489 equivalent (Asn284 of NdIS; Supplementary Table 1). The residues involved in the Ca^{2+}-binding site 2 were not conserved in NdIS.

The determined 4,206-nt-long DNA sequence contained two other partial open reading frames, *NdGH32A* and *NdGH68B*, neighboring the NdIS-coding gene (Fig. 4b). A DNA sequence with 96.5% identity was found in part of the gene cluster of the *Bacillus* sp. AFS031507 genome (Fig. 4c). The partial amino acid sequences of NdGH32A and NdGH68B corresponded to the C-terminal region (Asp362–Asp798) of the GH32 protein of the *Bacillus* strain (NCBI, WP_098930310.1), with 88.6% identity, and to the N-terminal region (Met1–Glu410) of GH68 (WP_098930308.1) with 98.9% identity. The *Bacillus* GH32 protein is similar to the GH32 enzymes, cycloinulooligosaccharide fructanotransferases (CFTs), and endo-inulinases, with approximately 40% sequence identity. The GH68 protein shows 31–40% identity with GH68 ISs and levansucrases.

Production of the recombinant NdIS in *E. coli*

Recombinant NdIS with a C-terminal His_6 tag was produced in *E. coli* BL21 (DE3) transformants

and purified by Ni^{2+}-immobilized affinity column chromatography to homogeneity by SDS-PAGE (Fig. 3a). Recombinant NdIS showed a slightly higher molecular mass than naive NdIS as expected with the addition of the C-terminal His_6 tag. A total of 8.4 mg of recombinant NdIS was obtained from 500 mL of shake-flask culture. Its specific activity (34.1 U/mg) was almost identical to that of the native enzyme (38.4 U/mg). The effects of pH and temperature on the activity and stability were similar to those of the native enzyme. The NdIS was most active at pH 6.1 and stable at a pH range of 5.1–8.1 (Fig. 6a). Its optimum temperature for activity was 40°C, but 45°C in the presence of 10 mM $CaCl_2$ (Fig. 6b). The temperature stability range at ≤ 40°C was not significantly changed by the addition of 10 mM $CaCl_2$ (Fig. 6c). No effect on enzymatic activity was observed in the presence of 10 mM EDTA (data not shown). Recombinant NdIS produced inulin-type polysaccharides from 400 mM sucrose, with a chain length distribution similar to that produced by the native enzyme (Fig. 2b).

Kinetic analysis of the reaction with sucrose

The initial reaction rates for aglycone release, hydrolysis, and transglycosylation were determined at various sucrose concentrations by colorimetric quantification of released D-glucose and D-fructose. The aglycone release and hydrolysis rates were almost identical up to 20 mM sucrose (Fig. 7a and b), indicating that the enzyme predominantly catalyzed hydrolysis against ≤ 20 mM sucrose. The reaction rate for transglycosylation increased with increasing substrate concentration. The three reaction rates followed well the rate equations (eq. 1–3) from the reaction scheme shown in Fig. 1 (Fig. 7a). The kinetic parameters determined were as follows: k_{cat1}, 22.6 ± 0.4 s^{-1}; k_{cat2}, 60.2 ± 0.4 s^{-1}; K_{m1}, 0.510 ± 0.06 mM; and K_{m2}, 918 ± 67 mM. The r_{tg} values determined at various sucrose concentrations followed Eq. 4. The transglycosylation parameter K_{TG}, which is the substrate concentration that provides the same rates of hydrolysis and transglycosylation, was 344 ± 19 mM (Fig. 7b).

Analysis of transglycosylates in the initial reaction

The kinetic analysis in the previous section was based on the D-glucose and D-fructose release rates. This leaves open the possibility that the reaction involves the transglycosylation products as acceptors even at the early stage of the reaction. In addition, the formation of unexpected products β-(2→1)-linked fructooligosaccharides was observed in the reaction by levansucrase (Crittenden and Doelle 1993; Euzenat *et al.* 1997). Therefore, the reaction products of recombinant NdIS were quantitatively analyzed. NdIS (50.4 nM) was almost 5 times higher than that used in the rate measurement in the previous section, and 800 mM sucrose was used as substrate. Products were detected with HPAEC-PAD (Fig. 8). 1-Kestose and D-glucose were detected as the major products, whereas D-fructose was detected as a minor product. No other trisaccharides were detected. In the 5-min reaction, the concentration of D-glucose (511 μM) was almost equal to the sum of the concentrations of D-fructose (125 μM) and 1-kestose (404 μM). These results indicated that, at 800 mM sucrose, transfructosylation was predominant, the transfructosylation acceptor was limited to sucrose, and no obvious transfructosylation was observed with 1-kestose as acceptor. In addition, NdIS catalyzed β-(2→1)-specific transfructosylation with sucrose even at the early stage of the reaction. The ratio of 1-kestose/sucrose concentrations (404 μM/800 mM) in the 5-min reaction is higher than the calculated 1-kestose/sucrose concentrations in the rate measurement in the previous section, mainly because of the reaction progress. No transfructosylation with 1-kestose acceptor even at the higher 1-kestose/sucrose ratio suggests that all the transglycosylation rates determined in the previous section occurred only with sucrose at all the concentrations.

Effect of sucrose concentration on the chain-length distribution of inulin-type polysaccharides

Recombinant NdIS catalyzes the production of inulin-type polysaccharides from 20–1,600 mM sucrose as the starting material. HPAEC-PAD analysis revealed that polysaccharides were produced as the reaction progressed, even with 20 mM sucrose (Fig. 9a). An insoluble product was observed in the reaction with 1,600 mM sucrose (Fig. 9b). The insoluble product dissolved rapidly upon heating to 100°C. The DPs of the most abundant polysaccharides from 20, 50, 100, 200, 400, 800, and 1,600 mM sucrose were 16, 21, 22, 22, 22, 22, and 18, respectively. From the concentrations of sucrose, D-fructose, and D-glucose in the reaction mixture, the ratios of sucrose consumed as donors and acceptors in the D-fructosyl transfer reaction were calculated. The ratio yielded average fructan DPs of 7.2, 12.1, 14.9, 16.5, 18.0, 18.2, and 14.3, when the initial sucrose concentrations were 20, 50, 100, 200, 400, 800, and 1,600 mM, respectively.

Discussion

Inulin is beneficial not only as a functional food ingredient, but also as a starting material for the production of functional oligosaccharides. IS, which catalyzes successive β-(2→1)-transfructosylation from sucrose to acceptors to synthesize β-(2→1)-fructan, is a promising enzyme for the mass production of inulin. In this study, we identified the soil bacterium *N. drentensis* 57N as an IS-producing bacterium, and investigated its enzymatic characteristics and amino acid sequences.

N. drentensis 57N produces NdIS extracellularly when cultured with sucrose as a carbon source, but not with D-glucose or D-fructose as the carbon source. No IS activity was detected in cell suspensions grown on any of the carbon sources tested. This indicates that *N. drentensis* 57N possesses no cell-associated IS, whereas the GH68 levansucrase from *Streptococcus salivarius* and IS from *S. mutans* GS-5 are produced in cell-associated forms (Milward and Jacques 1990; Rozen *et al*. 2004). Levansucrase localization varies with the carbon source in the culture medium. It is bound to the cell

wall with D-glucose, but released with sucrose (Milward and Jacques 1990). Cell-associated GH68 enzymes, including ISs from lactic acid bacteria, possess a cell-wall-anchoring C-terminal domain containing a PXX-repeat region, an LPXTG cell-wall-anchoring motif, and a hydrophobic stretch region (Rathsam *et al.* 1993; van Hijum *et al.* 2002), but NdIS has no additional domain. This was consistent with the finding that NdIS activity was detected only in the culture supernatant. The carbon source added to the culture medium regulates the production of NdIS, but not its localization. Sucrose induced NdIS production, whereas D-glucose and D-fructose suppressed it, presumably through carbon catabolite repression.

The *NdIS*-neighboring genes and the corresponding gene cluster in *Bacillus* sp. AFS031507 suggest that extracellularly produced β-(2→1)-fructan is assimilated by *N. drentensis* 57N as a carbon source, whereas fructan contributes to bacterial aggregation in *L. reuteri* TMW1.106 and *S. mutans* GS-5 (Walter *et al*. 2008; Rozen *et al.* 2004). The *NdIS*-flanking genes encode NdGH32A and NdGH68B, which presumably possess CFT/endo-inulinase and IS/levansucrase activities, respectively (Fig. 4b). The corresponding gene cluster of *Bacillus* sp. AFS031507 includes the genes encoding a putative extracellular GH68 enzyme (COE25_RS01260), a putative extracellular GH32 enzyme composed of two GH32 catalytic domains (COE25_RS31310), and ATP-binding cassette (ABC) transporter components (COE25_RS01305, _RS01310, and _RS01315) in addition to genes (COE25_RS01275, _RS01270, and _RS01265, respectively) corresponding to the three *N. drentensis* genes (Fig. 4c). Two GH32 proteins (COE25_RS31310 and _RS01275) were predicted to be extracellular and intracellular CFTs, respectively, owing to their high sequence similarity. Based on the possible activities, the metabolic pathway was predicted as follows: β-(2→1)-fructan is produced from sucrose by IS, then converted to cycloinulooligosaccharide by the extracellular GH32 CFT. Cycloinulooligosaccharides are imported into the cytosol by the ABC transporter and degraded by intracellular CFTs for further

metabolism.

Sequence comparisons of NdIS with GH68 enzymes revealed that the three catalytic residues and the residues involved in the direct interaction with substrates were highly conserved. To date, the complex structures of two ISs (InuHj and InuJ, Protein Data Bank entry, 7BJ4 [molecule B] and 2YFT, respectively) have been determined, and they show two significant differences in 1-kestose binding (Supplementary Fig. 2). The InuHj His82 equivalent is not present in InuJ because of the shorter 1B–1C region, but instead, Arg623 is situated in a similar position to form hydrogen bond with Fru O-6 at -1 subsite. The Glc moiety of 1-kestose binds differently to the +2 subsite as shown in Supplementary Fig. 2, with the different binding residues: Arg81, His82, His286 and Asn351 in InuHj and Arg542 and Arg545 in InuJ. NdIS shared almost all InuHj substrate-binding residues including the two His residues, although the whole sequence identity was only 33%. His112 and His335 are equivalent to His82 and His286 of InuHj, respectively. This suggested that NdIS accommodates 1-kestose in a manner similar to InuHj (Supplementary Fig. 2). The sole difference is Gln315 of NdIS at the position of Glu266 in InuHj, which interacts with the D-glucosyl moiety of sucrose and D-fructofuranosyl moiety of 1-kestose, respectively, in the +1 subsite. At this position, Glu is shared by the ISs of lactic acid bacteria and Gln by other ISs (Fig. 5). Ghauri *et al.* (2021b) reported that the Glu residue is carried by long-chain-synthesizing fructosyltransferases, whereas Gln is carried by relatively short-chain-synthesizing fructosyltransferases. In contrast, NdIS, which carries a Gln residue, synthesizes long-chain fructan polymers (Fig. 9).

NdIS does not require Ca^{2+} for its activity or stability. Its effect was limited by increasing the optimum temperature by 5°C (Fig. 6b, c). The effects of Ca^{2+} have been observed in many ISs from lactic acid bacteria, including InuJ (Anwar *et al.* 2008; Ozimek *et al.* 2005), but not in ISs from non-lactic-acid bacteria or archaea, including InuHj (Kralj *et al.* 2018; Frasch *et al.* 2017; Yokoi *et al.* 2021;

Ghauri et al. 2021a). Most of the Ca^{2+}-binding residues found in the InuJ structure are not conserved in the NdIS or in Ca^{2+}-independent ISs, including InuHj (Supplementary Table 1). This may explain the limited effect of Ca^{2+} on the NdIS. Ghauri *et al.* (2021a) suggested that a disulfide bridge (Cys226–Cys262) in InuHj partially compensates for the interactions via Ca^{2+} ions, but NdIS and other Ca^{2+}-independent ISs, except the *Streptomyces* enzyme HugO, have no Cys residues in the corresponding positions.

Kinetic analysis of the initial reaction rates of NdIS to sucrose showed that the NdIS reaction obeyed the reaction equation for retaining glycoside hydrolase, although other ISs were not analyzed using this reaction equation. NdIS catalyzed hydrolysis at low concentrations of sucrose (≤ 20 mM), but the transglycosylation ratio increased with increasing sucrose concentration, and the K_{TG} was 344 mM (Fig. 7). The high K_{TG} value clearly indicated that sucrose is an unfavorable acceptor substrate for NdIS. Although no obvious transglycosylation was detected at low substrate concentrations (Fig. 7), inulin-type polysaccharides were produced as the reaction progressed (Fig. 9). This suggests that sucrose serves predominantly as a donor substrate rather than an acceptor substrate, and the oligosaccharides formed slightly by transfructosylation act as superior acceptors. Due to the limited number of transglycosylation products, even at high concentrations of sucrose, long-chain fructans with DP42 or more were produced from 100 to 800 mM sucrose. This chain-length is higher than that of inulin-type polysaccharide (≤ DP27) synthesized from 100 to 800 mM sucrose by other *Bacillaceae* bacterial ISs, *Bacillus* sp. 217C-11 IS, InuO, and InuBK (Wada *et al.* 2003; Kralj *et al.* 2018; Yokoi *et al.* 2021). Multiple sequence alignment showed that the residues predicted to form the 1-kestose binding site were identical in NdIS and other ISs (Fig. 5). The structure of the ≥ +3 subsite and the differences in amino acid residues near the subsite may have changed the orientation, affecting substrate specificity, and changing the chain length of the product. To determine the mechanism for the synthesis of inulin-type

polysaccharides, the preference for acceptor substrates must be analyzed.

In this study, we isolated *N. drentensis* 57N from the soil as an inulin-type fructan-synthesizing bacterium and characterized its inulosucrase,NdIS. The NdIS showed high sequence similarity to reported ISs from non-lactic-acid bacteria, but produced fructan with a higher DP than these enzymes. Long-chain fructans are useful materials for DFA III synthesis, because DFA-III-producing inulin fructotransferases from *Arthrobacter pascens* T13-2 and *Bacillus* sp. snu-7 use fructooligosaccharides DP4 as substrates (Kang *et al.* 1998; Haraguchi *et al.* 2005). A water-insoluble product was generated during the reaction of NdIS with 1,600 mM sucrose, as observed in the reactions of InuHj from *H. jeotgali* B3T and IS from *L. reuteri* 121 (Ghauri *et al.* 2021a; Charoenwongpaiboon *et al.* 2019). The precipitated product of IS from *L. reuteri* 121, forms inulin nanoparticles and encapsulates flavonoids, such as quercetin and fisetin, to improve stability and water solubility (Charoenwongpaiboon *et al.* 2019). Inulin-type polysaccharides produced by NdIS presumably have a different structure from those of *L. reuteri* 121, in terms of their molecular mass and branch structure. Therefore, the water-insoluble fructan produced by NdIS is expected to have novel functions.

Authors' contributions

Y. K. and W. S. conducted the experiments and wrote the manuscript. T. N. and H. M. analyzed the data and wrote the manuscript.

Acknowledgments

We are grateful to Ms. Nozomi Takeda and Mr. Tomohiro Hirose of the Analysis Division, Global Facility Center, Creative Research Institution, Hokkaido University, for amino acid analysis. We thank Dr. Eri Fukushi of the GC-MS & NMR Laboratory, Research Faculty of Agriculture, Hokkaido

University, for NMR analysis.

Supplementary material

Supplementary material is available at Bioscience, Biotechnology, and Biochemistry online.

Data availability

The data supporting the findings presented in this article will be shared upon reasonable request from the corresponding authors.

Funding

This study received no specific grant from any funding agency.

Disclosure statement

No potential conflicts of interest are reported by the authors.

References

Altschul SF, Gish W, Miller W *et al*. Basic local alignment search tool. *J Mol Biol* 1990;**215**:403–410.

Anwar MA, Kralj S, van der Maarel MJ *et al*. The probiotic *Lactobacillus johnsonii* NCC 533 produces high-molecular-mass inulin from sucrose by using an inulosucrase enzyme. *Appl Environ Microbiol* 2008;**74**:3426–3433.

Armenteros JJA, Tsirigos KD, Sønderby CK *et al*. SignalP 5.0 improves signal peptide predictions using deep neural networks. *Nat Biotechnol* 2019;**37**:420–423.

Barrow GI, Feltham RKA. Cowan and Steel's manual for the identification of medical bacteria. 3rd

edition. Cambridge: University Press; 1993.

Batista FR, Hernández L, Fernández JR *et al*. Substitution of Asp-309 by Asn in the Arg-Asp-Pro (RDP) motif of *Acetobacter diazotrophicus* levansucrase affects sucrose hydrolysis, but not enzyme specificity. *Biochem J* 1999;**337**:503–506.

Bruker H III, Sims PF, Sinnott ML. Lignocellulose degradation by *Phanerochaete chrysosporium*: purification and characterization of the main α-galactosidase. *Biochem J* 1999;**339**:43–53.

Chambert R, Treboul G, Dedonder R. Kinetic studies of *Bacillus subtilis* levansucrase. *Eur J Biochem* 1974;**41**:285–300.

Chambert R, Gonzy-Treboul G. Levansucrase of *Bacillus subtilis.* Characterization of a stabilized fructosyl-enzyme complex and identification of an aspartyl residue as the binding site of the fructosyl group. *Eur J Biochem* 1976;**71**:493–508.

Charoenwongpaiboon T, Wangpaiboon K, Panpetch P *et al.* Temperature-dependent inulin nanoparticles synthesized by *Lactobacillus reuteri* 121 inulosucrase and complex formation with flavonoids. *Carbohydr Polym* 2019;**223**:115044.

Crittenden RG, Doelle HW. Structural identification of oligosaccharides produced by *Zymomonas mobilis* levansucrase. *Biotechnol lett* 1993;**15**:1055–1060.

Drula E, Garron ML, Dogan S *et al*. The carbohydrate-active enzyme database: functions and literature. *Nucl acids res* 2022;**50**:571–577.

del Moral S, Olivera C, Rodriguez ME *et al*. Functional role of the additional domains in inulosucrase (IslA) from *Leuconostoc citreum* CW28. *BMC Biochem* 2008;**9**:1–10.

Edelman J, Jefford TG. The mechanism of fructosan metabolism in higher plants as exemplified in *Helianthus tuberosus*. *New Phytol* 1968;**67**:517–531.

Euzenat O, Guibert A, Combes D. Production of fructo-oligosaccharides by levansucrase from *Bacillus*

subtilis C4. *Process Biochem* 1997;**32**:237–243.

Frasch HJ, van Leeuwen SS, Dijkhuizen L. Molecular and biochemical characteristics of the inulosucrase HugO from *Streptomyces viridochromogenes* DSM40736 (Tü494). *Microbiol* 2017;**163**:1030–1041.

Ghauri K, Ali H, Munawar N *et al.* Glycoside hydrolase family 68 gene of halophilic archaeon *Halalkalicoccus jeotgali* B3T codes for an inulosucrase enzyme. *Biocatal Biotransform* 2021a;**39**:206–213.

Ghauri K, Pijning T, Munawar N *et al.* Crystal structure of an inulosucrase from *Halalkalicoccus jeotgali* B3T-a halophilic archaeal strain. *FEBS J* 2021b;**288**:5723–5736.

Haraguchi K, Yoshida M, Ohtsubo K. Thermostable inulin fructotransferase (DFA III-producing) from *Arthrobacter* sp. L68-1. *Carbohydr Polym* 2005;**59**:411–416.

Hernandez L, Arrieta J, Menendez C *et al.* Isolation and enzymic properties of levansucrase secreted by *Acetobacter diazotrophicus* SRT4, a bacterium associated with sugar cane. *Biochem J* 1995;**309**:113–118.

Heyrman J, Vanparys B, Logan NA *et al. Bacillus novalis* sp. nov., *Bacillus vireti* sp. nov., *Bacillus soli* sp. nov., *Bacillus bataviensis* sp. nov. and *Bacillus drentensis* sp. nov., from the Drentse A grasslands. *Int J Syst Evol Microbiol* 2004;**54**:47–57.

Kang S, Kim W, Chang Y *et al.* Purification and properties of inulin fructotransferase (DFA III-producing) from *Bacillus* sp. snu-7. *Biosci Biotechnol Biochem* 1998;**62**:628–631.

Kawai R, Igarashi K, Kitaoka M *et al*. Kinetics of substrate transglycosylation by glycoside hydrolase family 3 glucan (1→3)-β-glucosidase from the white-rot fungus *Phanerochaete chrysosporium.* *Carbohydr Res* 2004;**339**:2851–2857.

Kirtel O, Lescrinier E, Van den Ende W, Toksoy Öner E. Discovery of fructans in Archaea. *Carbohydr*

Polym 2019;**220**:149–156.

Kobayashi M, Hondoh H, Mori H *et al*. Calcium ion-dependent increase in thermostability of dextran glucosidase from *Streptococcus mutans. Biosci Biotechnol Biochem* 2011;**75**:1557–1563.

Kralj S, Leeflang C, Sierra EI *et al*. Synthesis of fructooligosaccharides (FosA) and inulin (InuO) by GH68 fructosyltransferases from *Bacillus agaradhaerens* strain WDG185. *Carbohydr Polym* 2018;**179**:350–359.

Laemmli UK. Cleavage of structural proteins during the assembly of the head of bacteriophage T4. *Nature* 1970;**227**:680–685.

Livingston DP, Hincha DK, Heyer AG. Fructan and its relationship to abiotic stress tolerance in plants. *Cell Mol Life Sci* 2009;**66**:2007–2023.

Mach H, Volkin DB, Burke CJ *et al.* Ultraviolet absorption spectroscopy. *Methods Mol Biol* 1995;**40**:91–114.

Meng G, Fütterer K. Structural framework of fructosyl transfer in *Bacillus subtilis* levansucrase. *Nat Struct Mol Biol* 2003;**10**:935–941.

Milward CP, Jacques NA. Secretion of fructosyltransferase by *Streptococcus salivarius* involves the sucrose-dependent release of the cell-bound form. *J Gen Microbiol* 1990;**136**:165–169.

Moore S, Stein WH. Photometric ninhydrin method for use in the chromatography of amino acids. *J Biol Chem* 1948;**176**:367–388.

Morris C, Morris GA. The effect of inulin and fructo-oligosaccharide supplementation on the textural, rheological and sensory properties of bread and their role in weight management: A review. *Food Chem* 2012;**133**:237–248.

Nakagawa K, and Kawasaki H. DNA sequence analysis. In Society for Actinomycetes Japan (ed), Identification manual of Actinomycetes. Business Center for Academic Societies Japan, Tokyo, Japan

2001;83–117.

Niness KR. Inulin and oligofructose. *J Nutr* 1999;**129**:1402–1406.

Okuyama M, Serizawa R, Tanuma M *et al.* Molecular insight into regioselectivity of transfructosylation catalyzed by GH68 levansucrase and β-fructofuranosidase. *J Biol Chem* 2021;**296**:100398.

Olivares-Illana V, Wacher-Rodarte C, Borgne SL *et al*. Characterization of a cell-associated inulosucrase from a novel source: A *Leuconostoc citreum* strain isolated from Pozol, a fermented corn beverage of Mayan origin. *J Ind Microbiol Biotechnol* 2002;**28**:112–117.

Ozimek LK, Euverink GJW, van der Maarel MJEC *et al*. Mutational analysis of the role of calcium ions in the *Lactobacillus reuteri* strain 121 fructosyltransferase (levansucrase and inulosucrase) enzymes. *FEBS Lett* 2005;**579**:1124–1128.

Pijning T, Anwar MA, Böger M *et al*. Crystal structure of inulosucrase from *Lactobacillus*: insights into the substrate specificity and product specificity of GH68 fructansucrases. *J Mol Biol* 2011;**412**:80–93.

Ponstein AS, van Leeuwen MB. *In vitro* synthesis of inulin by the inulosucrase from *Streptococcus mutans. Studies in Plant Sci* 1993;**3**:281–287.

Pranznik W, Beck RHF. Application of gel permeation chromatographic systems to the determination of the molecular weight of inulin. *J Chromatogr A* 1985;**348**:187–197.

Rathsam C, Giffard PM, Jacques NA. The cell-bound fructosyltransferase of *Streptococcus salivarius*: the carboxyl terminus specifies attachment in a *Streptococcus gordonii* model system. *J Bacteriol* 1993;**175**:4520–4527.

Roberfroid M, Slavin J. Nondigestible Oligosaccharides. *Crit Rev Food Sci Nutr* 2000;**40**:461–480.

Roberfroid MB. Introducing inulin-type fructans. *Br J Nutr* 2005;**93**:13–25.

Robert X, Gouet P. Deciphering key features in protein structures with the new ENDscript server. *Nucl Acids Res* 2014;**42**:320–324.

Rosell KG, Birkhed D. An inulin-like fructan produced by *Streptococcus mutans*, strain JC2. *Acta Chem Scand B Org Chem Biochem* 1974;**28**:589.

Rozen R, Steinberg D, Bachrach G. *Streptococcus mutans* fructosyltransferase interactions with glucans. *FEMS Microbiol Lett* 2004;**232**:39–43.

Schägger H, Cramer WA, von Jagow G. Analysis of molecular masses and oligomeric states of protein complexes by blue native electrophoresis and isolation of membrane protein complexes by two-dimensional native electrophoresis. *Anal Biochem* 1994;**217**:220–230.

Shoaib M, Shehzad A, Omar M *et al*. Inulin: Properties, health benefits and food applications. *Carbohydr Polym* 2016;**147**:444–454.

Singh RS, Singh RP. Production of fructooligosaccharides from inulin by endoinulinases and their prebiotic potential. *Food Technol Biotechnol* 2010;**48**:435–450.

Song DD, Jacques NA. Purification and enzymic properties of the fructosyltransferase of *Streptococcus salivarius* ATCC 25975. *Biochem J* 1999;**341**:285–291.

Thompson JD, Higgins DG, Gibson TJ. CLUSTAL W: improving the sensitivity of progressive multiple sequence alignment through sequence weighting, position-specific gap penalties and weight matrix choice. *Nucleic Acids Res* 1994;**22**:4673–4680.

van Hijum SAFT, van Geel-Schutten GH, Rahaoui H *et al*. Characterization of a novel fructosyltransferase from *Lactobacillus reuteri* that synthesizes high-molecular-weight inulin and inulin oligosaccharides. *Appl Environ Microbiol* 2002;**68**:4390–4398.

Vergauwen R, Van Laere A, Van den Ende W. Properties of fructan: fructan 1-fructosyltransferases from chicory and globe thistle, two Asteracean plants storing greatly different types of inulin. *Plant Physiol* 2003;**133**:391–401.

Wada T, Ohguchi M, Iwai Y. A novel enzyme of *Bacillus* sp. 217C-11 that produces inulin from sucrose.

Biosci Biotechnol Biochem 2003;**67**:1327–1334.

Walter J, Schwab C, Loach DM *et al.* Glucosyltransferase A (GtfA) and inulosucrase (Inu) of *Lactobacillus reuteri* TMW1.106 contribute to cell aggregation, in vitro biofilm formation, and colonization of the mouse gastrointestinal tract. *Microbiol* 2008;**154**:72–80.

Yanase H, Maeda M, Hagiwara E *et al*. Identification of functionally important amino acid residues in *Zymomonas mobilis* levansucrase. *J Biochem* 2002;**132**:565–572.

Yokoi K, Tsutsui S, Arakawa G *et al.* Molecular and biochemical characteristics of inulosucrase InuBK from *Alkalihalobacillus krulwichiae* JCM 11691. *Biosci Biotechnol Biochem* 2021;**8**:1830–1838.

Yokota A, Hirayama S, Enomoto K *et al*. Production of inulin fructotransferase (depolymerizing) by *Arthrobacter* sp. H65-7 and preparation of DFA III from inulin by the enzyme. *J Ferm Bioe* 1991;**72**:258–261.

Table 1. Effects of 10 mM metal ions and EDTA on NdIS activity.

Salt	Activity (%)[a]
LiCl	103 ± 3
NaCl	100 ± 3
KCl	99 ± 2
NH_4Cl	100 ± 3
$MgCl_2$	102 ± 1
$CaCl_2$	112 ± 1
$CoCl_2$	51 ± 1
$NiCl_2$	35 ± 2
EDTA	99 ± 1

[a] Relative to activity in the absence of the metal ions. NdIS, inulosucrase from *Neobacillus drentensis* 57N

Fig. 1. Kinetic scheme of NdIS reaction on sucrose.

E, enzyme; Suc, sucrose; Kes, 1-kestose; E-Fru, fructosyl enzyme intermediate; NdIS, inulosucrase from *Neobacillus drentensis* 57N.

Fig. 2. Structural analysis of polysaccharide produced by NdIS.

(a) Thin-layer chromatography (TLC) analysis of reaction products from 333 mM sucrose using culture supernatant of *Neobacillus drentensis* 57N (lane 3) and by purified native NdIS (lane 5), and their digests by endo-inulinase (lanes 4, 6, respectively). Lanes 1, 2, inulin standard (Raftiline HP) and its digest by endo-inulinase, respectively. Lanes G, F, and S, D-glucose, D-fructose, and sucrose standards, respectively. (b) High-performance anion exchange chromatography-pulsed amperometric detection (HPAEC-PAD) analysis of the reaction products from 400 mM sucrose by native and recombinant NdIS. (c) ^{13}C-Nuclear magnetic resonance spectra of levan standard, inulin standard, and product of native NdIS from 400 mM sucrose.

Fig. 3. Electrophoretic analyses of native and recombinant NdIS.

(a) Sodium dodecyl sulfate polyacrylamide gel electrophoresis (SDS-PAGE). (b) Blue native PAGE. Lane N, native NdIS (1 μg); lane R, recombinant NdIS (1 μg); lane M, size markers. The molecular masses of the standards are shown on the left.

Fig. 4. Sequence analysis of the *NdIS* gene.

(a) Nucleotide sequence of the *NdIS* gene and its deduced amino-acid sequence. Amino-acid sequences determined by Edman degradation are underlined. The catalytic residues are in bold. (b) PCR-amplified DNA fragments and the partial gene cluster region including the *NdIS* gene determined in this study. (c)

The gene cluster in *Bacillus* sp. AFS031507 containing the *NdIS*-corresponding region (indicated with a double arrow) of the 68_C3_Contig1_140404 data. Locus tags (last 5 digits following "COE25_RS") and annotated functions or domains of the gene products are shown. UK, unknown.

Fig. 5. Multiple sequence alignment of characterized inulosucrases.

InuHj, inulosucrase (IS) from the archaeon *Halalkalicoccus jeotgali* B3T; NdIS, IS from *Neobacillus drentensis* 57N; InuO and InuBK, IS from the *Bacillaceae, Salipaludibacillus agaradhaerens* WDG185 and *Alkalihalobacillus krulwichiae* JCM11691, respectively. HugO, IS from *Streptomyces viridochromogenes* DSM 40736. IS from the lactic acid bacteria indicated with asterisks: *Lactobacillus johnsonii* NCC533 (InuJ), *L. gasseri* DSM20604, *L. reuteri* 121, *L. reuteri* TMW 1.106, *L. jensenii* JV-V16. IS from *Streptococcus mutans* GS-5, *Weissella confusa* MBFCNC-2 (1), and *Leuconostoc citreum* CW28. FF*Zm*, LS*Zm,* β-fructofuranosidase, and levansucrase were obtained from *Zymomonas mobilis* ATCC29191. Stars: catalytic residues (Nu: nucleophile; TS: transition-state stabilizer; A/B: acid/base). Black arrowheads indicate amino acid residues that form subsites -1, +1, and +2 of InuHj for 1-kestose binding. White arrowheads indicate residues that form subsites -1 and +2 in InuJ from *L. johnsonii*, but are not conserved in NdIS. Circles indicate residues that determine the regioselectivity of transfructosylation in FF*Zm* and LS*Zm*. The strand notation was based on Ghauri *et al.* (2021b).

Fig. 6. Effects of pH and temperature on activity and stability.

(a) Effects of pH on activity at 37°C (filled circle) and remaining activity after incubation at 4°C for 24 hours (open circle). (b) Activity measured at the indicated temperatures at pH 6.5 in a 10-min reaction in the absence (filled circle) and presence of 10 mM $CaCl_2$ (open circle). (c) Residual activity after incubation at the indicated temperatures at pH 6.5 for 15 min in the absence (filled circle) and presence

of 10 mM $CaCl_2$ (open circle). The results are presented as the means of triplicate experiments with standard deviations.

Fig. 7. Kinetics of catalytic reaction toward sucrose.

(a) The dependence of initial velocities of aglycone release (v_{ag}, filled circle), hydrolysis (v_h, open circle), and transglycosylation (v_{tg}, filled triangle) on sucrose concentration. (b) Dependence of transglycosylation ratio ($r_{tg} = v_{tg}/v_{ag}$) on sucrose concentration. Theoretical curves with the kinetic parameters are drawn. The data are presented as the means of triplicate experiments with standard deviations.

Fig. 8. HPAEC-PAD analysis of the initial reaction products of NdIS from 800 mM sucrose.

The reaction was performed in 800 mM sucrose and 50.4 nM recombinant NdIS. The reaction products were analyzed at 0–10 min intervals. The standards included 20 mg/L of D-glucose, D-fructose, sucrose, and 1-kestose. G, D-glucose; F, D-fructose; S, sucrose; K, 1-kestose.

Fig. 9. Degree of polymerization distributions of reaction products of recombinant NdIS from various concentrations of sucrose (a) and appearance of the reaction solution (b).

The reactions were carried out with 20–1,600 mM sucrose and the products were analyzed using HPAEC-PAD. The degree of polymerization (DP) of the reaction products are shown at the top of the figure.

Supplementary Table 1. Comparison of amino acid residues of the Ca^{2+}-binding site 1 of InuJ with corresponding residues of InuHj and NdIS.

InuJ	InuHj	NdIS
Asp419	Met191	Ile227
Gln450	Ile219	Arg257
Trp487	Glu233	Leu282
Asn489	Asn235	Asn284
Asp521	Gln265	His314

NdIS, inulosucrase from *Neobacillus drentensis* 57N; InuJ, inulosucrase from *Lactobacillus johnsonii* NCC533; InuHj, inulosucrase from *Halalkalicoccus jeotgali* B3T

Supplementary Fig. 1. Profiles of hydrophobic interaction chromatography of native NdIS.

A Toyopearl Butyl 650M column was used. Filled circle, A_{280}; open circle, D-glucose-releasing activity; filled triangle, ammonium sulfate concentration.

Supplementary Fig. 2. 1-Kestose binding site of the crystal structures of InuHj (a) and InuJ (b).

The structures of InuHj (Protein Data Bank entry, 7BJ4, molecule B) and InuJ (2YFT) in a complex with 1-kestose are shown. 1-Kestose is in yellow. The amino acid residues involved in the interaction with 1-kestose are indicated. The predicted hydrogen bonds between the residues and 1-kestose are indicated by red dashed lines. The equivalent residues of NdIS are indicated in parentheses in panel (a).

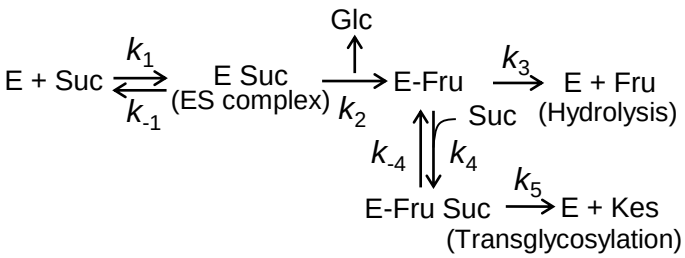
Glc
E + Suc
k_1
k_{-1}
E Suc
(ES complex)
k_2
E-Fru
k_3
E + Fru
(Hydrolysis)
Suc
k_{-4}
k_4
k_5
E-Fru Suc
E + Kes
(Transglycosylation)

Figure 1

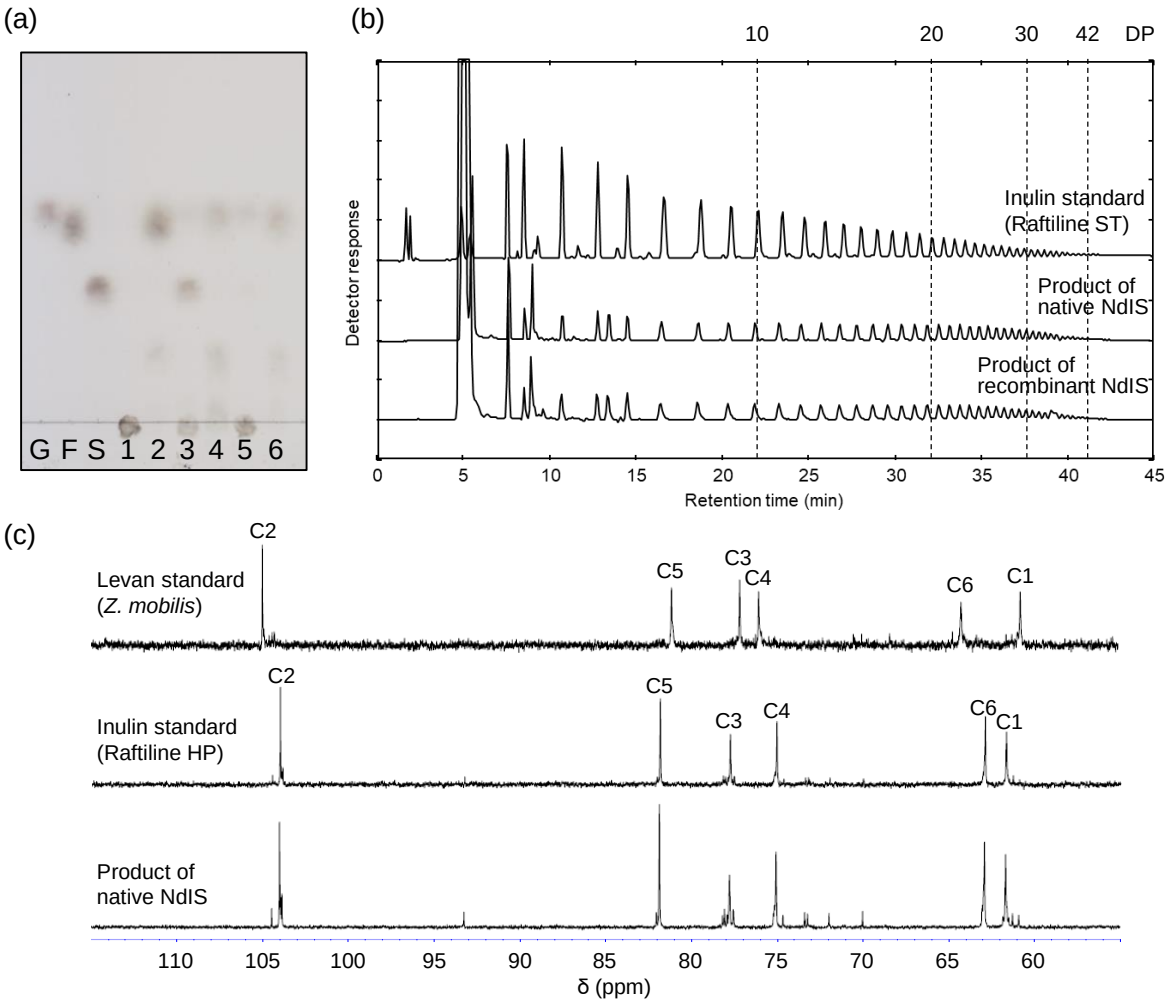
(a)
G F S 1 2 3 4 5 6
(b)
10
20
30
42
DP
Detector response
Inulin standard
(Raftiline ST)
Product of
native NdIS
Product of
recombinant NdIS
0
5
10
15
20
25
30
35
40
45
Retention time (min)
(c)
Levan standard
(Z. mobilis)
C2
C5
C3
C4
C6
C1
Inulin standard
(Raftiline HP)
Product of
native NdIS
110
105
100
95
90
85
80
75
70
65
60
δ (ppm)

Figure 2

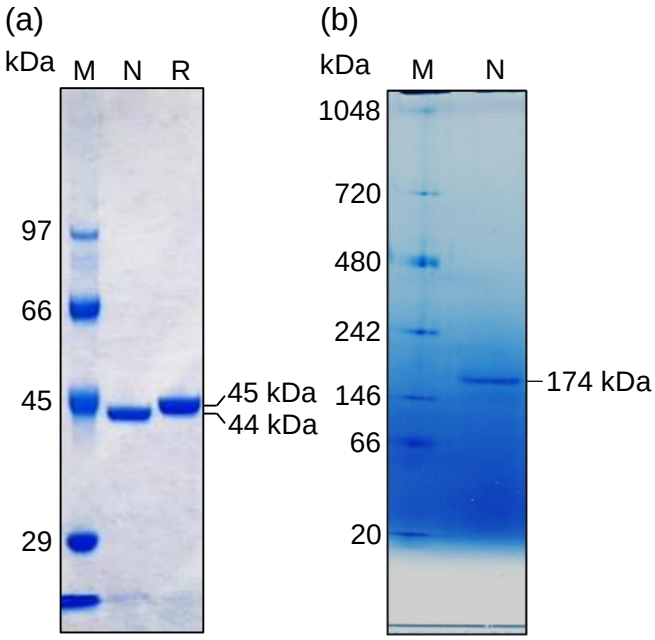
(a)
kDa
M
N
R
97
66
45
29
45 kDa
44 kDa
(b)
kDa
M
N
1048
720
480
242
146
66
20
174 kDa

Figure 3

(a)

```
ATGGAAATGAAAACTCGTAACAAATCGAAATTGAAAAAGCTGGTTTTGACAGCCGTTGTTGCTGTCAATTGCCTGTCAGTAACACAAGCA   90
 M  E  M  K  T  R  N  K  S  K  L  K  K  L  V  L  T  A  V  V  A  V  N  C  L  S  V  T  Q  A    30
TTTGCAGCGGAAATCAGTTCAGATTACACATCCATCTGGTCACGTCAGCAAGCAGAAAAAGTAACGCCTACTGACAAAACAACAGCACCG  180
 F  A  A  E  I  S  S  D  Y  T  S  I  W  S  R  Q  Q  A  E  K  V  T  P  T  D  K  T  T  A  P    60
AAAATTGATCTTGATTTTGATCTTGTAGCACCTGATCAATGGGTATGGGATACATGGCCATTACAAAATAGAGATGGTTCAATGGCGATT  270
 K  I  D  L  D  F  D  L  V  A  P  D  Q  W  V  W  D  T  W  P  L  Q  N  R  D  G  S  M  A  I    90
GTCAATGGCTACCGAGTGGCCTTTGCATTGGTAGCACCGCGTTCTTTAGGATGGGGTGAGCGCCATACAGAAGCAAGAATTGGAATGTTC  360
 V  N  G  Y  R  V  A  F  A  L  V  A  P  R  S  L  G  W  G  E  R  H  T  E  A  R  I  G  M  F   120
TACTCCAAGAACGGCAAAGATTGGACGTACGCAGGAATCCCTTATGACTATAATAAAGCCTTGGGGCATATGCAATGGGCCGGAACAGCA  450
 Y  S  K  N  G  K  D  W  T  Y  A  G  I  P  Y  D  Y  N  K  A  L  G  H  M  Q  W  A  G  T  A   150
ATGCTTGATGACAATGGAAAAGTTCATTTATTCTATACGGCAACCGGTGAAAAAACAAATTGGGATAACAATGGATGGGATAAAAGAGCC  540
 M  L  D  D  N  G  K  V  H  L  F  Y  T  A  T  G  E  K  T  N  W  D  N  N  G  W  D  K  R  A   180
GTACAGCGGATTGCGAAAACAACCTTTGATATTCATACGGATAAAAACGGGGTTCATCTGACCAATGAAGGGAAACATCAAGTCATTCTT  630
 V  Q  R  I  A  K  T  T  F  D  I  H  T  D  K  N  G  V  H  L  T  N  E  G  K  H  Q  V  I  L   210
GAAGCAGATGGAAAATATTACGAGACACTTGCACAAGCGAATAGTCCGATCATTACGGCATTCCGTGATCCATTCTTCTTCCAGGATCCG  720
 E  A  D  G  K  Y  Y  E  T  L  A  Q  A  N  S  P  I  I  T  A  F  R  D  P  F  F  F  Q  D  P   240
AATACAGGCAAAGAGTATATTATCTTCGAAGGACAAGCTGGAAGCGATAGAGACTTTATCAAACCGGAAAATATCGGGGATGAAGAATAC  810
 N  T  G  K  E  Y  I  I  F  E  G  Q  A  G  S  D  R  D  F  I  K  P  E  N  I  G  D  E  E  Y   270
CGCAAAACCCATTCCGTTCCTGCAGGAGCCGAATTGTATAACGGTAATATCGGGATCGCAGAAGTACTTGACAAAGACGTAACCAAATTA  900
 R  K  T  H  S  V  P  A  G  A  E  L  Y  N  G  N  I  G  I  A  E  V  L  D  K  D  V  T  K  L   300
AAGCTTCTCCCGCCATTGCTTGAGTCGGTTGGAACCAATCACCAGATGGAACGTCCGCACATGGTCGTAAACGGAGATGATTATTATCTA  990
 K  L  L  P  P  L  L  E  S  V  G  T  N  H  Q  M  E  R  P  H  M  V  V  N  G  D  D  Y  Y  L   330
TTTACCATCAGCCATACCTTTACGTATGCTCCTGGCTTGACTGGTCCTGATGGTGTCTATGGATTTGTTGGTAAAGGACTGTTCGGCAGC 1080
 F  T  I  S  H  T  F  T  Y  A  P  G  L  T  G  P  D  G  V  Y  G  F  V  G  K  G  L  F  G  S   360
CATAAACCAATGAATGAAAGTGGTCTTGTGATTGCGAATCCAAAGGAAAGCCCTTATCAAGCCTATTCTTGGATGGTTCTTCCAGACCAG 1170
 H  K  P  M  N  E  S  G  L  V  I  A  N  P  K  E  S  P  Y  Q  A  Y  S  W  M  V  L  P  D  Q   390
CAGGTAATCAGCTTTATTAACGAGCCGAAAGATGAGAACGGTAATGTGAAATTTGGCGGTACATTCGCCCCAACTCTAAAAGTGAAGCTG 1260
 Q  V  I  S  F  I  N  E  P  K  D  E  N  G  N  V  K  F  G  G  T  F  A  P  T  L  K  V  K  L   420
AATGGCGAAACATCTGAAGTTGTAAAAGAAGGTAAAGCGGGCGAAATTAAACCATTTGGGGCAAATCGCTAA                    1332
 N  G  E  T  S  E  V  V  K  E  G  K  A  G  E  I  K  P  F  G  A  N  R Stop                    443
```

(b) *N. drentensis* 57N

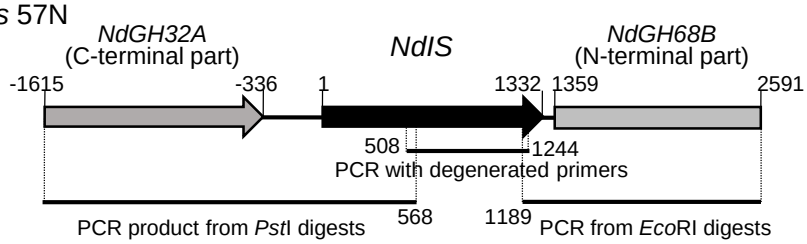

(c) *Bacillus* sp. AFS031507

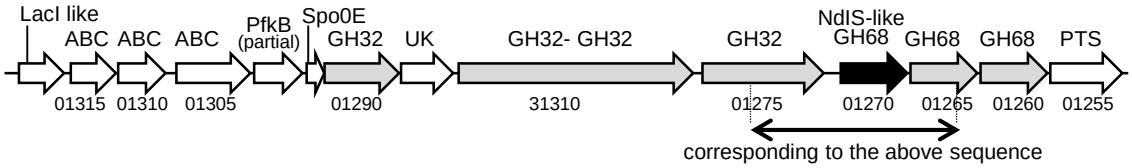

Figure 4

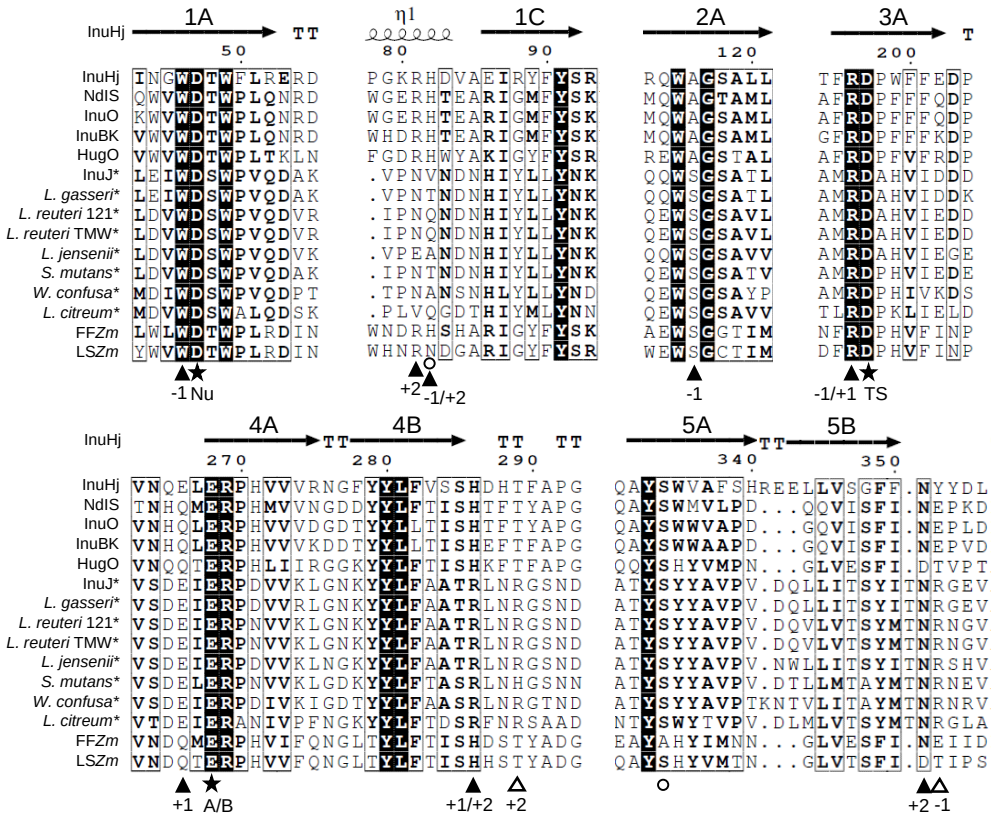
InuHj
1A
TT
ηl
1C
2A
3A
T
50
80
90
120
200
InuHj
NdIS
InuO
InuBK
HugO
InuJ*
L. gasseri*
L. reuteri 121*
L. reuteri TMW*
L. jensenii*
S. mutans*
W. confusa*
L. citreum*
FFZm
LSZm
-1 Nu
+2
-1/+2
-1
-1/+1 TS
4A
4B
5A
5B
270
280
290
340
350
+1 A/B
+1/+2
+2
+2 -1

Figure 5

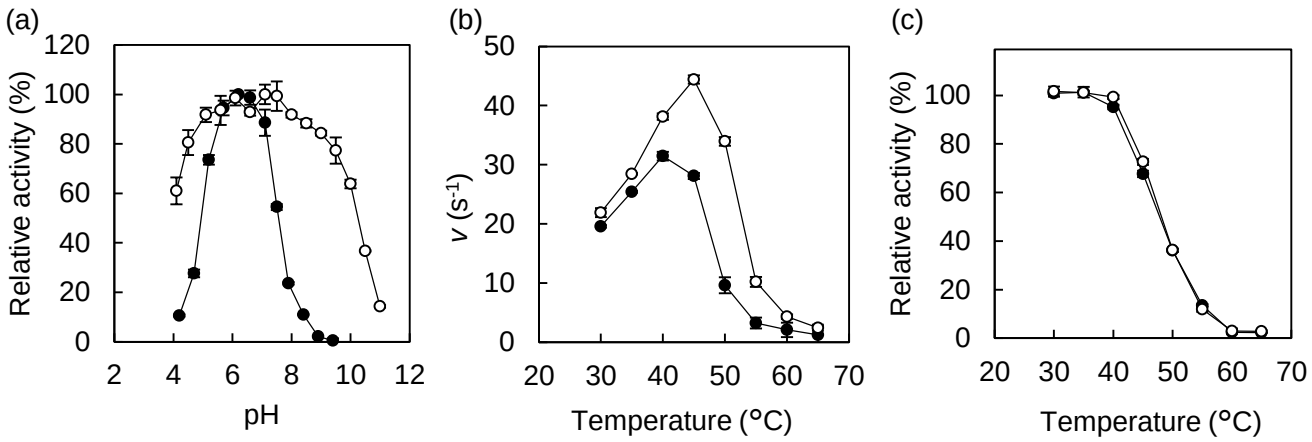
(a)
Relative activity (%)
120
100
80
60
40
20
0
2
4
6
8
10
12
pH
(b)
v (s-1)
50
40
30
20
10
0
20
30
40
50
60
70
Temperature (°C)
(c)
Relative activity (%)
100
80
60
40
20
0
20
30
40
50
60
70
Temperature (°C)

Figure 6

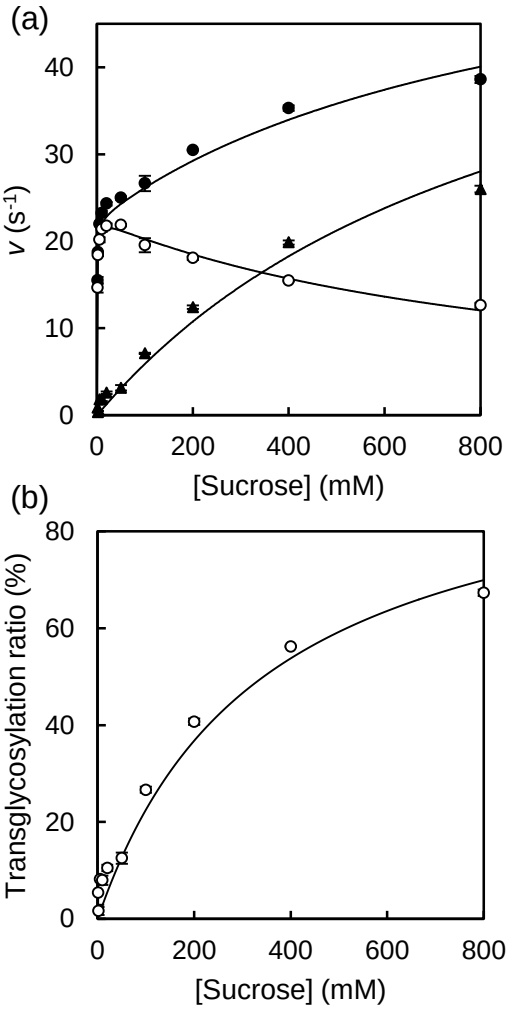
(a)
40
30
20
10
0
v (s-1)
0
200
400
600
800
[Sucrose] (mM)
(b)
80
60
40
20
0
Transglycosylation ratio (%)
0
200
400
600
800
[Sucrose] (mM)

Figure 7

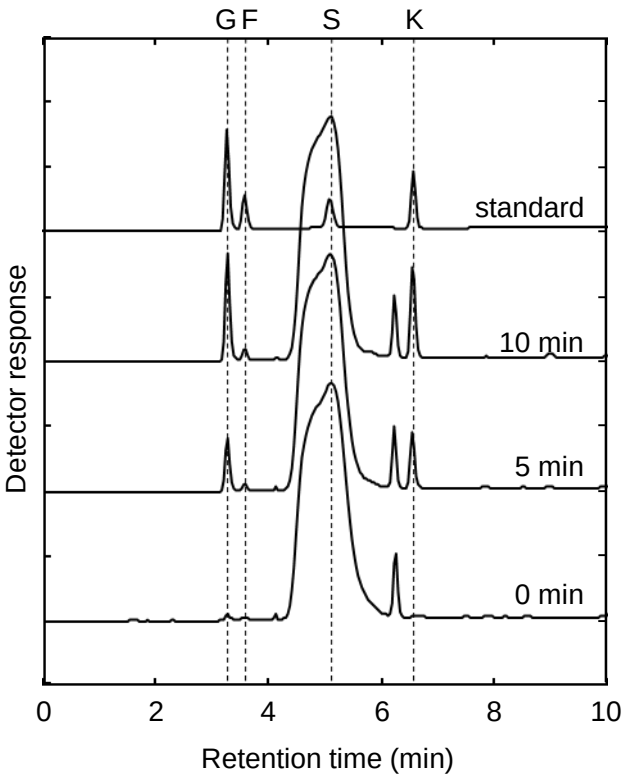
G F
S
K
standard
10 min
5 min
0 min
Detector response
0
2
4
6
8
10
Retention time (min)

Figure 8

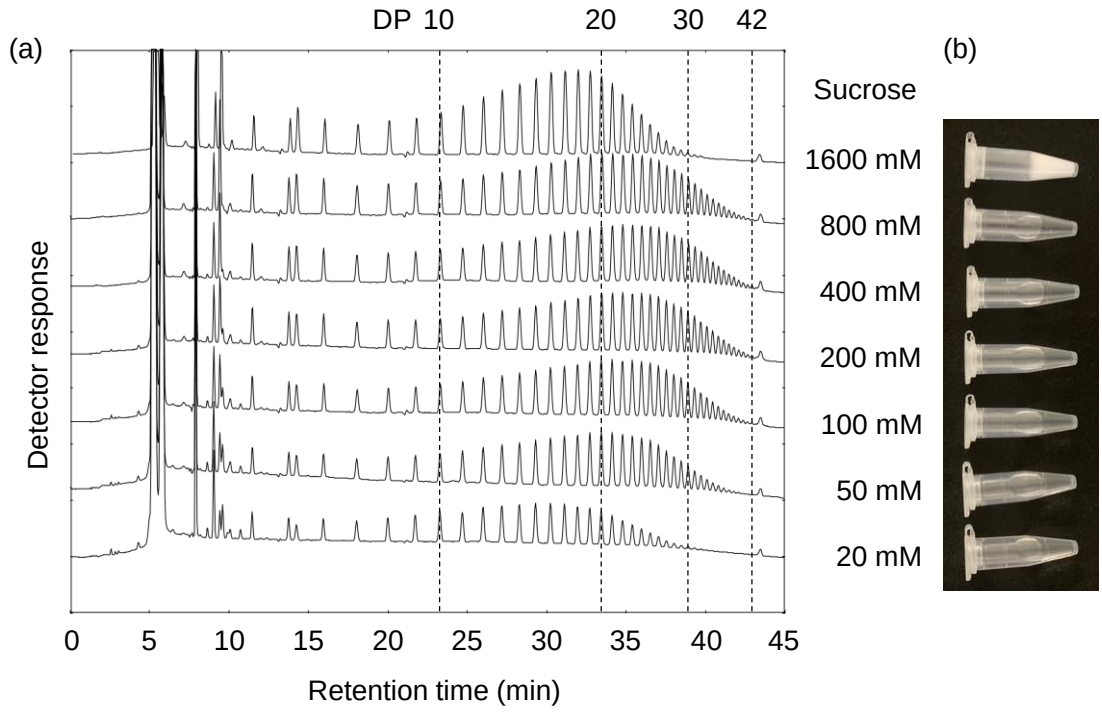
(a)
DP 10
20
30
42
Sucrose
1600 mM
800 mM
400 mM
200 mM
100 mM
50 mM
20 mM
Detector response
0
5
10
15
20
25
30
35
40
45
Retention time (min)
(b)

Figure 9